Journal of Information Systems Engineering and Management
2025, 10(26s)
e-ISSN: 2468-4376
https://www.jisem-journal.com/

Research Article

Deep Learning-Based Single Image De-Raining Using Discrete Hartley Transformation

Nibedita Patra[1*], Chinmayee Dora A[2], S.S. Nayak[3]
[1*]*Research Scholar, Department of Electronics and telecommunications Engineering*
Centurion University of Technology and Management
Paralakhemundi, Odisha 761211
2Assistant Professor, Department of electronics and Communications Engineering,
Centurion University of Technology and Management
Bhubaneswar, 752050
[3]*Professor in Physics, Department of Physics*
Centurion University of Technology and Management
Paralakhemundi, Odisha 761211
[1*]*Corresponding Email: nibu.mallik@gmail.com*

ARTICLE INFO

Received: 28 Dec 2024

Revised: 10 Feb 2025

Accepted: 28 Feb 2025

ABSTRACT

In computer vision, the removal of rain streaks from individual photographs has drawn a lot of interest. A saturated picture is broken down to an underlying image without any rain and a map of the rain streak to represent the de-raining challenge as an image decomposition assignment. This study introduced a DLD: Deep Learning-Based Single Image De-Raining Using Discrete Hartley Transformation, which is different from the majority of de-raining techniques now in use. The data cleansing phase of this study uses contrast-limited adaptive histogram equalization to smooth out the image and lower noise. Then, we introduced a new method to reconstruct a rainy image called Discrete Hartley Transformation (DHT). Following that feature extraction is carried by the proposed Deep Learning-based Enhanced Share-Source Residual Module (SSRM) which improves image performance also its shortcut connections. Finally, the Inverse Discrete Hartley Transformation (IDHT) is used to de-rained images. As a result, our proposed method achieves a high accuracy of 93.6, PSNR of 41.9, and SSIM of 0.96 compared to the existing techniques.

Keywords: Image de-raining, Deep residual learning, Image processing, Single image.

1. INTRODUCTION

With a method developed, it is possible to swiftly execute the Discrete Hartley Transform (DHT) of a data sequence of N elements in a time equivalent to N log 2 N. Error-avoiding inverse Hartley transforms are equivalent to the original Hartley transform. Rain is a typical weather occurrence. Raindrops may result in the outside computer vision system operating abnormally, blurring the obtained outdoor picture, losing the image's original details and characteristics, and lessening the image's visual impact. For instance, the fields of image enhancement, monitoring targets, recognition, and de-raining algorithms are all very helpful in ensuring the overall correctness of the method. De-raining algorithms for images have gained popularity recently.

The project of decomposing a rainy image into a backdrop image devoid of rain and a rain streak map is known as the de-raining challenge. Rain streaks can cause problems for a wide range of image-based uses throughout the modern world, such as self-driving vehicles operation, satellite-based photo monitoring, tracking, etc. It may also be interpreted as a challenge to effectively reduce noise in a single picture or video. Rain streak reduction from one picture is an image decomposition problem where a rainy image is split into a backdrop image with no precipitation and a map of the rain streaks. In computer vision, a lot of study has been done on removing rain streaks from single photos. The conventional method of removing rain from a single image interprets each raindrop as a distinct type of high-frequency noise, which is subsequently filtered using either the raindrop recognition approach or the image decomposition technique. Numerous kinds of rain removal procedures have been introduced one after the other.

Recent research has revealed that rain streaks may be eliminated from a single picture using spatial domain techniques. Fu et al. [1, 2] developed a network based on negative residual learning (ResNet)[3] utilizing a Deep Residual Network. This network may be used to rainy photos to obtain their de-rained versions. Prior to picture de-raining, Shen et al. [4] employed the ideas of Haar [5], wavelets, and Dark channels [6]. [7,8,9] The authors have proposed networks that use apriori information, which includes (a) centralized sparse representation, (b) depending on anticipated rain direction, (c) rain streak layer, and (d) Gaussian mixture theories, to remove a rain map from a wet picture to produce a backdrop devoid of rain. Zhang et al. [10] develop the low-rank representation-based convolutional kernels with rain streaks and sparsity in order to recognize the clear images. Applying bilateral filtering, a grainy image is separated into its high-frequency and low-frequency components [11-15]. The high-frequency component is then further separated into geometric features associated with rain and non-rain. It is the histogram was produced using a structured dictionary learning of Eigen colors, depth of field, and horizontally oriented gradients (HOG).

The periodic noise that follows is extracted by Chang et al.[16] byline patterns like fences, stripes, and raindrops. Al. [18] introduced the Chun et al model, which depends on the Conditional Generative Adversarial Network [17] to compute the high-quality image of no rain. Gu et al's [19] work describes the decomposition of the rainy image into two layers: one layer is approximated by sparse modeling study to depict large-scale structures, and the other layer is determined by sparse illustration synthesis to display the finer textures in the image and eliminate the rain streaks. A model that simultaneously identifies and eliminates rain streaks utilizing a binary map was proposed by Yang et al. [20]. The rain streak is visible in the pixel if the proper value in the binary map is"1," otherwise it is "0." They can mimic heavy rain by mimicking the appearance of rain stripe accumulation in different shapes and orientations. Ren et al.'s [21] model of the rain streaks, which is separated into heavy and sparse rain, makes use of a matrix decomposition framework. Yeh et al. [22] divide an image of rain into its high- and low-frequency components using Gaussian filter.

Rain streaks from low-frequency components are eliminated using non-negative matrix factorization, whereas rain streaks from high-frequency components are eliminated using astute edge recognition. Wang et al. [23] developed a framework that utilized the observation that most of the rain streaks are located in high-frequency component of rainy picture. The rain-free information from high-frequency component is learned through a dictionary-based technique. Applying a Convolutional Neural Network (CNN) is difficult because many useful features, like the local receptive field, are lost when an image's spectrum is in the Fourier domain, according to Shen et al. [24]. We proposed a DLD: Deep Learning-Based Single picture De-Raining Utilizing a Discrete Hartley Transformation method to enhance picture efficiency in order to overcome the shortcomings of earlier studies. The following is a summary of our work's primary efforts:

- For image reconstruction, existing research used Discrete Fourier Transform (DFT), but it degrades the performance, thus we introduced a new method to reconstruct a rainy image called Discrete Hartley Transformation (DHT).
- In addition, we proposed the SSRM, a modified residual design, in which every shortcut connection has a common beginning point. This modification to the original ResNet may accelerate convergence and improve the acquisition of the de-rained output.
- To improve the accuracy of the introduced SSRM this research utilized Group normalization(GN) and Sigmoid function which smooth the gradient, much more flexible and better to handle. The proposed strategy may remove rain effectively and efficiently, according to findings from experiments.

This research article is organized this way: After reviewing artificial intelligence-based picture de-raining in Section 2, Section 3 provides a detailed description of the proposed research. The findings of the proposed technique's implementation were shown in Section 4. The study's work is concluded in Section 5.

2. LITERATURE SURVEY

To prevent catastrophic forgetting, Zhou et al. [25] introduced the parameter significance guided weights modifying method, or PIGWM, for the picture de-raining community. This approach is able to preserve the efficiency of the prior rain dataset while achieving satisfactory results. A possible method has been devised that shares the network design but updates and stores the network's settings on every set of data individually. To capitalize on picture prior and strong feature mapping, there is a propensity to combine data-driven and model-driven techniques.

In order to retrieve contextual data along the global spatial dimensions and channel dimensions, Fu et al. [26] initially suggested two GCN blocks after introducing a dilated convolution block to record multi-scale local patterns along the local spatial dimensions. Tests confirm this approach's superiority on simulated and actual information sets. Furthermore, our network structure exhibits good computational effectiveness, de-raining performance, and ease of implementation.

In order to extract clear picture material from a single rainy picture, Yang et al. [27] suggested eliminating rain elements without adding any new artifacts. The rain element is frequently modelled as noise in current rain removal techniques. It is suggested to use a Rain-Component-Aware (RCA) network to record the rain's properties. The suggested method might yield far superior de-raining photographs with regard to both subjective visual quality inspection and objective quantitative assessment. The RCA network is good at collecting rain patterns.

In order to achieve outstanding de-raining effectiveness without the need for expensive pre-training, Xiao et al. [28] presented a successful transformer-based framework for the picture de-raining fundamental priors of vision tasks, i.e., locality and hierarchy, into the design of the network. Methods for de-raining have to find features that are both local and non-local. Strong dependencies between content and position can thus be gathered, improving image content recovery and minimizing precipitation artifacts.

An effective de-raining unit and a deep de-raining CNN were proposed by Yao et al. [29]. Utilizing a feature pyramid, we acquire knowledge of rain streaks with varying sizes and forms. We then utilize these features in the de-raining unit, propagating them across the network to facilitate learning of the deep de-raining network and enhance its general efficiency.

An adaptive-kernel pyramid was developed by Zhang et al. [30] to effectively deliver multi-scale data. Then, to search for channel and spatial links among two scales, accordingly, we develop two cross-scale similarity attention blocks (CSSABs). While the channel CSSAB highlights the interdependencies among cross-scale features, the spatial CSSAB investigates the spatial similarity among pixels of cross-scale parameters. Lastly, we build an efficient multifocal attention-based cross-scale system using our CSSABs that achieves image de-raining by fully utilizing the cross-scale correlations of both rain streaks and background.

Wang et al. [31] introduced a two-step technique called JF-MADN that consists of a Multi-scale deep Alternate-connection Dense Network (MADN) that separates rain streaks in a coarse-to-fine way and a Joint Filter (JF) that extracts high-frequency features from pictures taken during rainy conditions. To divide the high-frequency and low-frequency elements of the rainy picture, a rain-prior weighted statistic order filter might be built by integrating it with the rain dark channel prior.

Using several public datasets, Wei et al. [32] presented an approach, and the experimental findings show that this suggested approach significantly improves image de-raining and de-blurring. One of the key data sources in IoV is the transportation images. This study studies the image de-blurring and image de-raining methods using DL and transfer learning that retrieve traffic information from motion-blurred and rain-damaged images. To attain higher accuracy in the image de-blurring task, a motion de-blurring technique depending on deep residual generation adversarial network with our own created Res-block is offered.

Hence, Discrete Fourier transformation (DFT) is used to reconstruct the rainy image in the existing research. In order to simulate the rain streak map in the Fourier domain, both the phase and magnitude spectrums are needed. Actual and unreal coefficients are supplied as input to the deep network in place of magnitude and phase data in order to lower the cost of computation. Because of the signal transformation's loss of spatial correlation, transform domain images are useless for deep network training. Moreover, Noise will affect the reconstruction. Our current research proposes a periodic or pseudo-periodic structure, which remains a few marks in the altered domain, but decreases the noise. Also, deep CNN is used to modify rain streaks in an image. For that D-Net and N-Net are used to estimate and predict the rain streaks, moreover, the performance is decreased.

3. DLD: DEEP LEARNING-BASED SINGLE IMAGE DE-RAINING USING DISCRETE HARTLEY TRANSFORMATION

To increase picture efficiency, a brand-new DLD: Deep Learning-Based Single picture De-Raining Utilizing Discrete Hartley Transformation method is put out. First, the input is the picture of the rain. Generally, input image is affected by some noise. So, the data are cleansed by Contrast-limited adaptive histogram equalization which reduces the noise,

smoothens the image, and performs well in terms of periodic noise. Moreover, the existing research used Discrete Fourier Transform (DFT), but it degrades the performance, thus we introduced a new method to reconstruct a rainy image called Discrete Hartley Transformation (DHT). In addition, to extract features, the existing research employed different types of neural networks with different amounts of layers to estimate and predict the images, still, it takes more time to process and it affects the classification performance. So, to overcome the above-mentioned flaws, we proposed a Deep Learning-based Enhanced Share-Source Residual Module (SSRM), and it improves image classification performance also its shortcut connections. Here, to improve the accuracy, this research introduced Enhanced SSRM which comprises Group normalization (GN) and Sigmoid function that smooth the gradient, much more flexible and better to handle. Finally, the Inverse Discrete Hartley Transformation (IDHT) is used to de-rained images. Figure 1 shows the architecture of the proposed strategy.

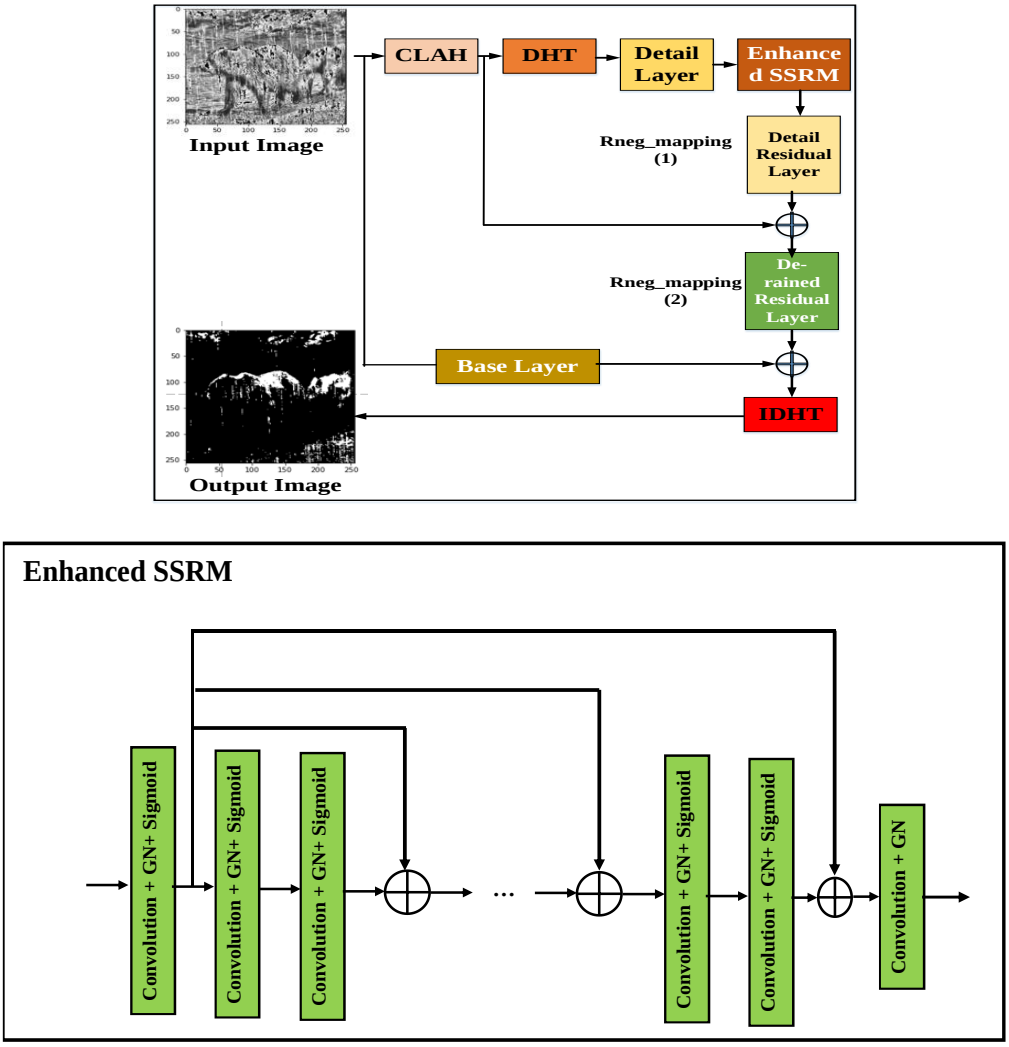

Figure 1: Architecture of the proposed approach

3.1 PCLAHE: Pre-processing by Contrast limited adaptive histogram equalization

This research adopts the PCLAHE method to increase the visibility and reduce the noises in the input image. The process of PCLAHE presented in Figure 2, is composed of two major parts:

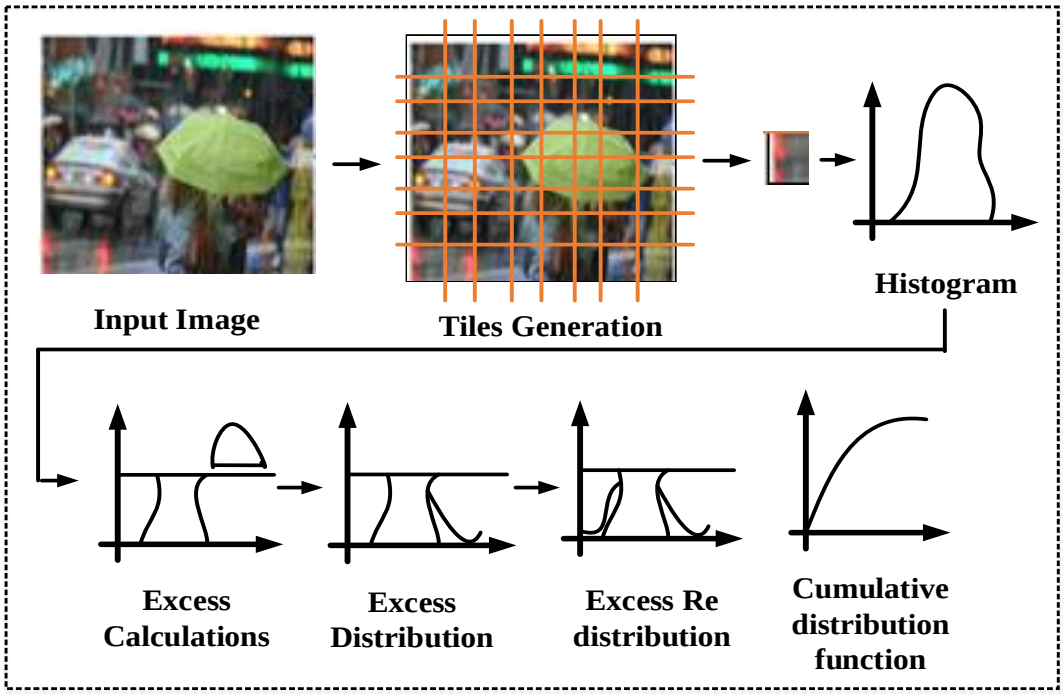

Figure 2: Pre-processing method that employs contrast-limited adaptive histogram equalization

A contrast factor known as a clip limit is used by CLAHE to clip (that is, cap or clip) the histogram in order to avoid oversaturation of the picture, particularly in homogeneous regions. Adaptive histogram clip (AHC), a version on the contrast-limited method, is another tool for controlling the over-enhancement of picture backgrounds. By modifying the clipping level, it functions. Typically, one of the AHCs that yields a bell-shaped graph is the Rayleigh distributions. Here is how the function is specified:

$$Rayleigh_g = g_{min} + \left[2(\alpha^2)\ln\left(\frac{1}{1-p_f}\right)\right]^{0.5}$$

A minimum pixel value is indicated by g_{min} in this function. The distribution parameter, α, is a positive real scalar that specifies the cumulative probability distribution, represented as p_f.

Algorithm 1: PCLAHE: Pre-processing by Contrast limited adaptive histogram equalization
Tile generation: Partitioning the input image into non-overlapping blocks or tiles is the first stage. For each tile, a histogram is calculated. This histogram represents the distribution of pixel intensities within that specific tile.
Histogram equalization: There are five steps in this section:
❖ **Histogram computation:** Determine the histogram as a collection of bins on every tile.
❖ **Excess calculation:** Compile the values of the histogram bins that surpass the clip limit.
❖ **Excess distribution:** After that, divide them among other containers.
❖ **Excess redistribution:** A more successful clip restriction that is greater than the stated limit—whose precise value depends on the image—will be possible thanks to the redistribution, which will push some bins back above the clip limit. Execute the redistribution process iteratively until the excess is minimal if this is not what you want.
❖ **Scaling and mapping:** Determine the values of the histogram's cumulative distribution function (or CDF). Next, use the input image pixel values to scale and map every tile's CDF values.

Hence, PCLAHE performs well in terms of periodic noise. Following that, the existing research used Discrete Fourier Transform (DFT) for reconstructing a rainy image, but it degrades the performance, thus we introduced a novel approach which is explained in the following section.

3.2 IRDHT: Image Reconstruction by Discrete Hartley Transformation (DHT)

A 2D DHT pair is described below in order to propose a DHT reconstruction for a rainy image:

$$H(u,v) = \sum_{x=0}^{M-1}\sum_{y=0}^{N-1} f(x,y) cas\left[2\pi\left(\frac{ux}{M}+\frac{vy}{N}\right)\right] \quad (1)$$

$$f(x,y) = \sum_{x=0}^{M-1}\sum_{y=0}^{N-1} H(u,v) cas\left[2\pi\left(\frac{ux}{M}+\frac{vy}{N}\right)\right] \quad (2)$$

Where H (u, v) is the Hartley spectrum coefficient; M and N are the pre-processed picture's horizontal and vertical dimensions, accordingly; and f (x, y) indicates the pre-processed images; and $cas(\theta) = cos(\theta) + sin(\theta) = \sqrt{2}\, sin(\theta + \pi/4)$. Equations (1) and (2) can therefore alternatively be written in the form of:

$$H(u,v) = \sum_{x=0}^{M-1}\sum_{y=0}^{N-1} f(x,y)\left(cos\left[2\pi\left(\frac{ux}{M}+\frac{vy}{N}\right)\right] + sin\left[2\pi\left(\frac{ux}{M}+\frac{vy}{N}\right)\right]\right) \quad (3)$$

$$f(x,y) = \sum_{x=0}^{M-1}\sum_{y=0}^{N-1} H(u,v)\left(cos\left[2\pi\left(\frac{ux}{M}+\frac{vy}{N}\right)\right] + sin\left[2\pi\left(\frac{ux}{M}+\frac{vy}{N}\right)\right]\right) \quad (4)$$

By simplifying it, we can further obtain

$$H(u,v) = \sqrt{2}\sum_{x=0}^{M-1}\sum_{y=0}^{N-1} f(x,y) sin\left[2\pi\left(\frac{ux}{M}+\frac{vy}{N}\right)+\pi/4\right] \quad (5)$$

$$f(x,y) = \sqrt{2}\,\frac{1}{MN}\sum_{x=0}^{M-1}\sum_{y=0}^{N-1} H(u,v)\, sin\left[2\pi\left(\frac{ux}{M}+\frac{vy}{N}\right)+\pi/4\right] \quad (6)$$

This approach uses a specific formula for creating the fringe illumination patterns p(.) of various spatial frequencies:

$$p(x,y;u,v) = a + bsin(2\pi ux + 2\pi vy + \pi/4)$$

Where (u,v) are the spatial frequencies of the illumination structures, (a) is the DC component, and (b) is the contrast; a and b are used to control the brightness of the illumination patterns. Where (x,y) are the 2D Cartesian coordinates in the target pre-processed image. The target pre-processed image is then projected with the illumination structures, and a number of distinct voltage signals are found and captured utilising a single detector. The expression for a reflection modulation signal Dp is as follows:

$$D_p(u,v) = D_n + k\iint R(x,y)p(x,y;u,v)dxdy \quad (7)$$

where k is a constant whose value is determined by the location as well as the dimensions of the detector, R is the surface albedo of the target pre-processed image, and D_n is the intensity of the ambient light. When we plug Eq. (7) into Eq. (8), we obtain

$$D_p(u,v) = D_n + ak\iint R(x,y)\, dxdy + bk\iint R(x,y)\, sin(2\pi ux + 2\pi vy + \pi/4)dxdy \quad (8)$$

This approach has a high signal-to-noise ratio and is also differential. The element of DC may be removed by averaging all the data, as demonstrated by the Fourier series theory, once all the basic designs have been added together to create a consistent pattern. D_p and $\widehat{D}$ stand for the voltage signals and the average of all the data, accordingly. It is possible to retrieve every spectral coefficient of the recreated picture by utilizing the subsequent formula is:

$$H(u,v) = D_p - \widehat{D} \quad (9)$$

Every Hartley spectral coefficient of the recreated picture is calculated using Eq. (10). Lastly, a 2D inverse DHT can be used for getting the reconstructed picture. Then, to extract the features and de-rained the image this research proposed a novel approach which is explained in the following section.

3.3 Deep Learning-based Enhanced Share-Source Residual Module (SSRM)

The current research utilized various neural network types with varying numbers of layers to forecast and estimate the pictures in order to extract the features; however, this approach takes longer to process resulting in worse classification performance. Thus, to overcome the above-mentioned flaws, this research proposed a Deep Learning Enhanced Share-Source Residual Module (SSRM), in which ResNet-50 and Bottleneck Dense Net (Dense Net-B) are utilized and it improves image classification performance also its shortcut connections. In order to speed up convergence along with enhance data flow among layers, SSRM was developed. Additionally, in order to enhance the computation for every residual block, it will make use of an identical source and pre-identify a variable. Moreover, to improve the accuracy, this research introduced an Enhanced SSRM which comprises Group normalization (GN) and Sigmoid function that smooth the gradient, much more flexible and better to handle.

The rainy picture, or reconstructed picture from the DHT, may be divided into two sections: the detail layer and the base layer. The detail layer may be represented statistically as follows:

$$R = R_{base} + R_{detail} \quad (10)$$

In this case, the subscripts 'detail' and 'base' stand for the detail and base levels, accordingly, while R is the rainy picture. The detail level is sparser than the rainy picture since all that's left in R_{detail}, are rain streaks along with partially constructed object architecture. Instead of training the SSRM on the image domain, we do so on the detail layer.

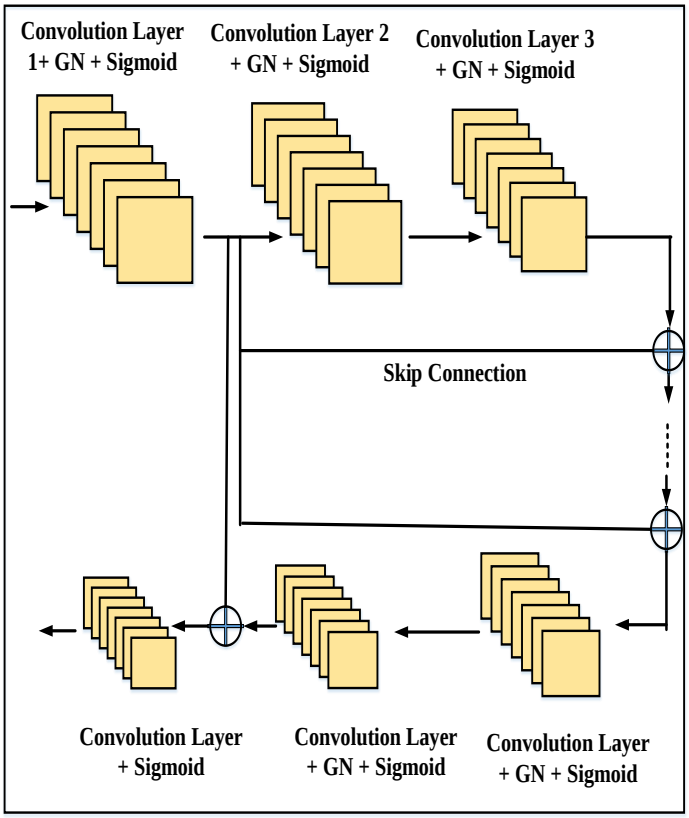

Figure 3: Structure of Enhanced SSRM

Comparing the SSRM with N layers to a normal CNN, Figure 3 illustrates that the N-layered SSRM has (N-2)/2 residual blocks and shortcut connections. Furthermore, by having every shortcut link have an identical source, the SSRM's foundation's adaptability and integrity are reinforced. As a result, while each leftover block is unique, they

are all connected. It is possible to transfer feedforward and feedback signals directly using these shortcut connections. First, this research explained about the enhanced SSRM which is explained as follows:

As shown in Figure 3, if we set I^0 as the input image from the DHT, I_{in}^n and I_{out}^n correspondingly symbolize the SSRM's inputs and outcomes in the n^{th} layer. After then, the SSRM's architecture can be summed up as below:

$$\begin{cases} I_{in}^1 = I^0 \\ I_{out}^1 = \sigma(\mathrm{GN}(W^1 * I_{in}^1 + b^1)) \end{cases} \tag{11}$$

$$\begin{cases} I_{in}^2 = I_{out}^1 \\ I_{out}^2 = \sigma(\mathrm{GN}(W^2 * I_{in}^2 + b^2)) \\ I_{in}^3 = I_{out}^2 \\ I_{out}^3 = \sigma(\mathrm{GN}(W^3 * I_{in}^3 + b^3)) \end{cases} \tag{12}$$

$$\begin{cases} I_{in}^4 = I_{out}^3 + I_{out}^1 \\ I_{out}^4 = \sigma(\mathrm{GN}(W^4 * I_{in}^4 + b^4)) \\ I_{in}^5 = I_{out}^4 \\ I_{out}^5 = \sigma(\mathrm{GN}(W^5 * I_{in}^5 + b^5)) \end{cases} \tag{13}$$

$$\begin{cases} I_{in}^{2n} = I_{out}^{2n} + I_{out}^1 \\ I_{out}^{2n} = \sigma(\mathrm{GN}(W^{2n} * I_{in}^{2n} + b^{2n})) \\ I_{in}^{2n+1} = I_{out}^{2n} \\ I_{out}^{2n+1} = \sigma(\mathrm{GN}(W^{2n+1} * I_{in}^{2n+1} + b^{2n+1})) \end{cases} \tag{14}$$

$$\begin{cases} I_{in}^N = I_{out}^{N-1} + I_{out}^1 \\ I_{out}^N = \sigma(\mathrm{GN}(W^N * I_{in}^N + b^N)) \end{cases} \tag{15}$$

The overall amount of layers N is represented by the variable $n = 1, 2, \ldots, (N-2)/2$. The sigmoid function is denoted by σ(.), the convolution operator by *, the weight parameters by W, the bias by b, and the group normalization function by GN(.). Two filters are used following the upgraded SSRM process: the detail residual level & the de-rained residual level, which are described below:

As shown in Figure 1, this research chose two filters to minimize $R_{neg-mapping1}$(detail residual layer) which are formulated as

$$R_{neg-mapping1} = C - R_{base} - R_{detail} \tag{17}$$

Initially, the optimized R_{base}^* is obtained by a low-pass filter and can be expressed as

$$R_{base}^* = \underset{R_{base}}{\mathrm{argmin}}(C - R_{base}) \tag{18}$$

Similarly, we use a high-pass filter to extract R_{detail}^0 detail according to the identified R_{base}^*.

$$R_{detail}^0 = \underset{R_{detail}}{\mathrm{argmin}}((C - R_{base}^*) - R_{detail}) \tag{19}$$

Ultimately, we find the best $R_{neg-mapping1}$ using the formulas (17)–(19), which significantly streamlines the training procedure. Rain streaks tend to appear white in pictures, hence rainy image R has greater pixel values than clean image C. This is referred to as "negative residual mapping" because the majority of C-R ratios often have a negative value.

Depicted in figure 1, $R_{neg-mapping1}$ (detail residual layer) and $R_{neg-mapping2}$ (de-rained residual layer) to increase the effectiveness of image decomposition, two negative residual mappings are constructed. Initially, we generate the de-rained residual layer $R_{neg-mapping2}$ by learning the residual values across the final picture C and the base layer R_{base}. This may be represented as

$$R_{neg-mapping2} = C - R_{base}^* \tag{20}$$

The detailed residual level $R_{neg-mapping1}$ is then obtained by learning the residual across $R_{neg-mapping2}$ and detail layer R_{detail}. This can be expressed as,

$$R_{neg-mapping1} = R_{neg-mapping2} - R^0_{detail} \quad (21)$$

$$R_{neg-mapping1} = f^b_w(R^0_{detail}) \quad (22)$$

Where $R_{neg-mapping1}$ signifies the outcome of SSRM, and $f^b_w(.)$ symbolizes the SSRM. Finally, the Inverse Discrete Hartley Transformation (IDHT) is used to de-rained images. In the following section, this research presents the implementation results of the proposed approach to show its effectiveness.

4. RESULTS AND DISCUSSION

An 8 GB RAM Python framework was used to train our algorithm. In order to verify the efficacy of our algorithm, we assessed our procedure using the current image-draining techniques.

4.1 Dataset Description

The JRDR De-raining dataset, which is available to the public on Kaggle, is the primary dataset used in this work. Among the artificial data sets for images are (1) Rain dataset heavy, which contains 200 training pairs and 100 ground-truth testing pairs; (2) Rain 100 light, which contains 200 training synthetic pairs and 100 testing and ground-truth testing pairs, accordingly.

Table 1: Dataset Details

Description	Training Sets	Testing Sets
Datasets of heavy rain images	200	100
Datasets of light rain images	200	100

4.2 Obtained results from the proposed approach

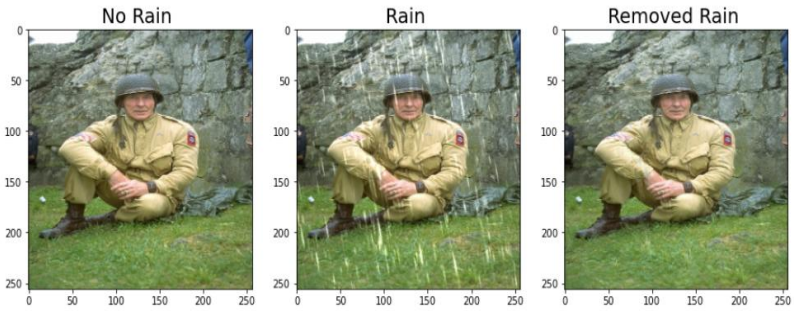

Figure 4: Obtained result from the heavy rain (Sample 1)

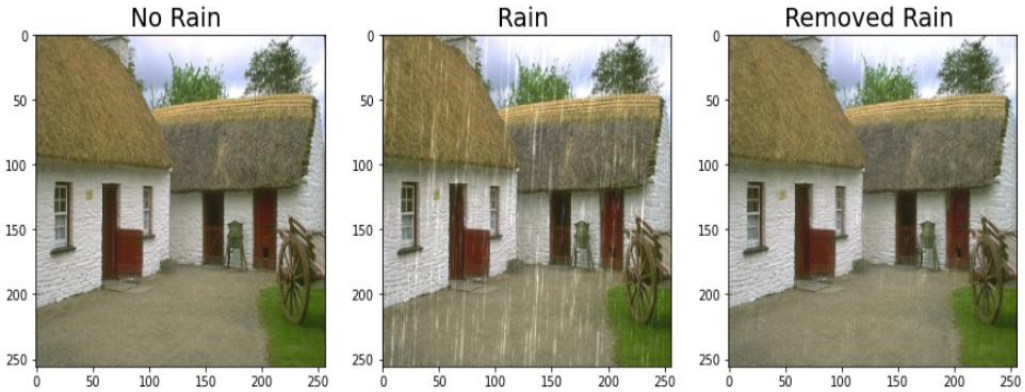

Figure 5: Obtained result from the heavy rain (Sample 2)

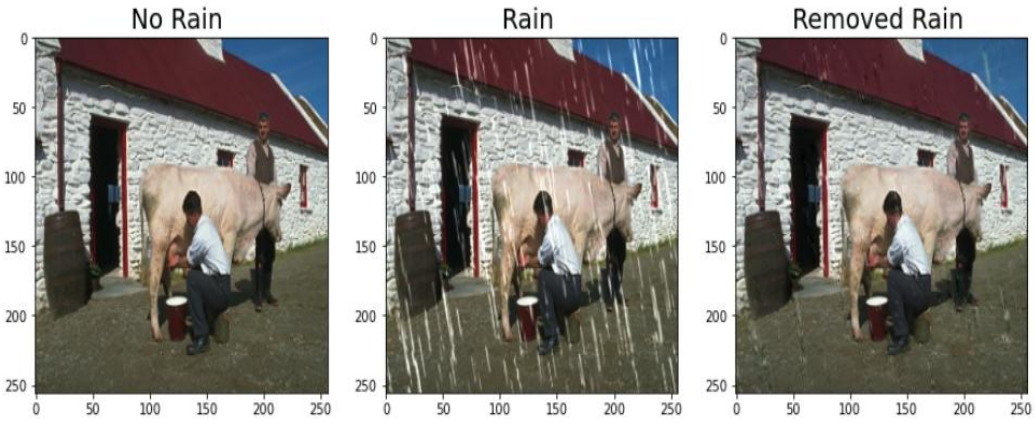

Figure 6: Obtained result from the heavy rain (Sample 3)

Three artificial high-rainy pictures are visualized in Figure 6-8, where two places of interest have been chosen to display high-rain streaks. Specifically, the proposed DLD: In severe rain, the rain streaks were successfully eliminated by DL-Based Single Image De-Raining Utilizing Discrete Hartley Transformation.

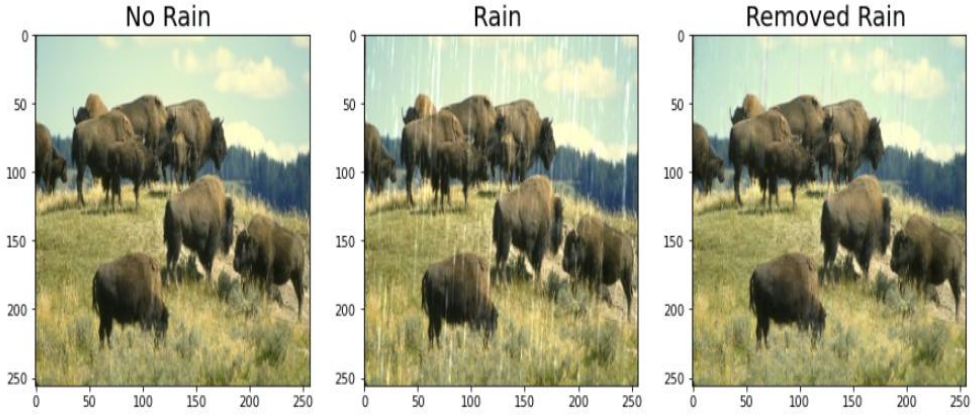

Figure 7: Obtained result from the light rain (Sample 1)

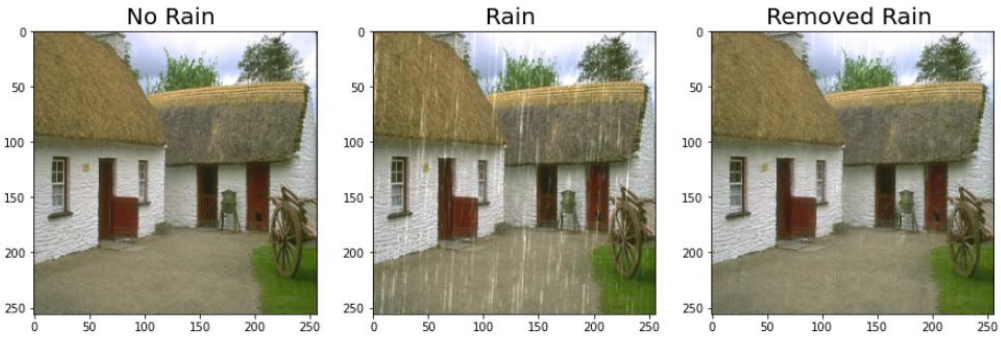

Figure 8: Obtained result from the light rain (Sample 2)

Two synthetic light rainy views are depicted visually in Figure 9-10; light-rain streaks are picked in two places of interest. Specifically, the proposed DLD: Discrete Hartley Transformation-Based Deep Learning-Based Single Image De-Raining was successful in eliminating the rain streaks in light rain.

4.3 Performance parameters

The performance specifications of the proposed DLD are explained in the part: Discrete Hartley Transformation-Based Deep Learning-Based Single Image De-Raining Technique. The total accurateness of the model's predictions is measured by accuracy. It gives a general picture of performance by calculating the proportion of accurately

anticipated occurrences to all instances. Furthermore, the difference among the expected and actual values is represented by the loss. Loss functions quantify this difference mathematically. The aim is to minimize this loss, as a lower loss signifies a more accurate mode.

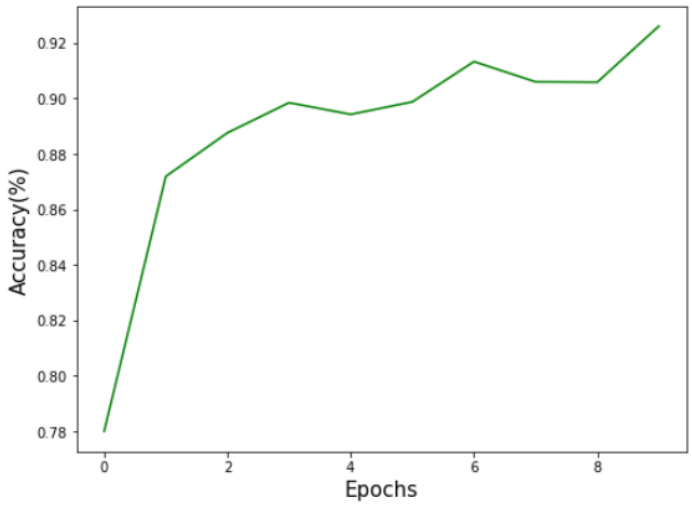

Figure 9: Accuracy of the proposed approach

The accuracy of the proposed method over epochs is displayed in Figure 11. One full cycle across the entire training dataset is referred to as an epoch. Through every epoch, the model learns from the entire dataset, adjusting its parameters to minimize the difference between predicted outputs and actual targets. Multiple epochs are necessary to ensure that the model has seen the data sufficiently and has fine-tuned its weights and biases to make accurate predictions.

In the early epochs of training, the model's accuracy might be relatively low. This is because the model starts with random weights and biases and does not yet understand the underlying patterns in the data. As training progresses through several epochs, the model refines its understanding of the data. Accuracy typically improves during this phase. Greater forecasts are produced as the algorithm begins to identify more complex patterns and correlations in the dataset.

The relationship between accuracy and epochs illustrates the model's learning curve. It starts with low accuracy and improves as the model learns from the data. Hence, our proposed approach attains an accuracy of 93.6% in the 8th epoch.

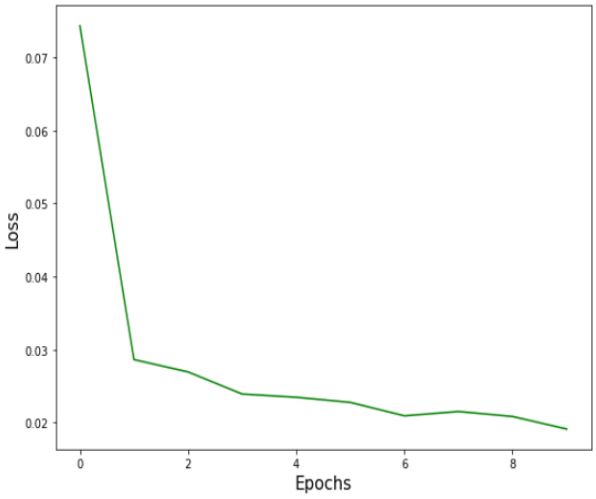

Figure 10: Loss of the proposed approach

Loss is a gauge of the model's effectiveness. As seen in Figure 12, it estimates the discrepancy among the target numbers in the training dataset with the projected outputs. Reducing this loss function is the aim of training. A lower

loss suggests an improved fit between the model and the training set of data since its forecasts are more in line with the real data.

Usually, the model has a large loss during the initial epoch of training. This is because the model does not recognize the patterns in the data because its parameters are set up at random. As the training progresses through multiple epochs, the model learns from the data and adjusts its parameters to minimize the loss. With each epoch, the loss gradually decreases, indicating that the model is becoming better at making predictions. As a result, our proposed approach provides a 0.02 loss in 8th epochs.

4.4 Comparison Analysis

In our experiments, we are able to assess every method using two widely-used quantitative measurements: the structural similarity index (SSIM) and the peak signal-to-noise ratio (PSNR) for pictures that have ground truth. Greater picture recovery quality is indicated by bigger PSNR and SSIM values.

PSNR is typically expressed in decibels (dB). The formula for PSNR is:

$$PSNR = 10 \times \log_{10}\left(\frac{MAX^2}{MSE}\right)$$

Where MSE is the Mean Squared Error across the initial and processed pictures and MAX is the highest feasible pixel value of the picture. Since PSNR uses a logarithmic function, it is measured in decibels (dB). The visual distortion decreases as the PSNR value increases.

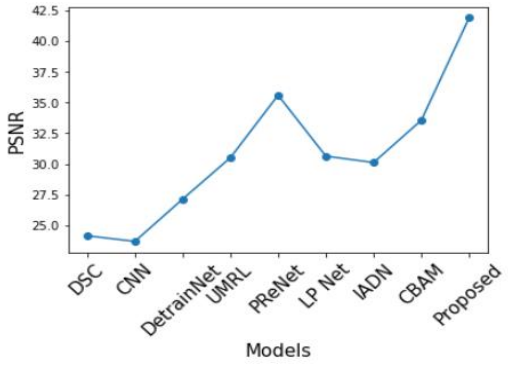

Figure 11: Comparison of PSNR

Figure 13 compares the general Peak Signal Noise Ratio (PSNR). By employing contrast-limited adaptive histogram equalization, or Discrete Hartley Transformation, the proposed method's PSNR increases. Our proposed approach attains higher PSNR when compared to the baseline as Deep Spatial Context (DSC), Convolutional Neural Network (CNN), DetrainNet, Unrolled Matching Recursive Learning (UMRL), Progressive Image Restoration Network (PReNet), Low-light Image Processing Network (LP Net), Invertible Auto encoding Decentralized Network (IADN), and Convolutional Block Attention Module (CBAM) such as 24.6%, 23.9, 26.6, 30.2, 35.3, 32.6, 32.5, and 33.9. As a result, our novel technique has a PSNR of 41.9, which is higher than baseline approaches.

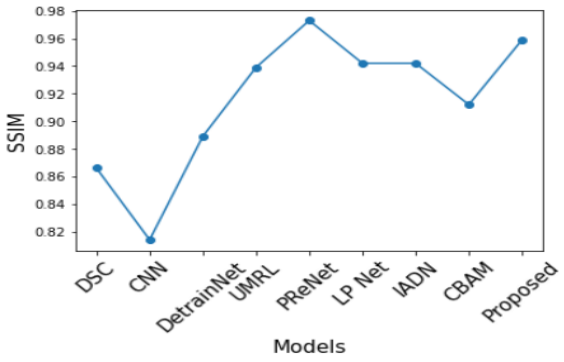

Figure 12: Comparison of SSIM

The overall Structural Similarity Index (SSIM) comparison is exposed in Figure 13. The SSIM of the proposed technique improves by using contrast-limited adaptive histogram equalization - Discrete Hartley Transformation. Our proposed approach attains higher SSIM when compared to the baseline as Deep Spatial Context (DSC), Convolutional Neural Network (CNN), DetrainNet, Unrolled Matching Recursive Learning (UMRL), Progressive Image Restoration Network (PReNet), Low-light Image Processing Network (LP Net), Invertible Auto encoding Decentralized Network (IADN), and Convolutional Block Attention Module (CBAM) such as 0.87, 0.816, 0.882, 0.932, 0.94, 0.948, 0.943, and 0.917. As a result, our novel technique has an SSIM of 0.96 which is higher than baseline approaches.

As an outcome, compared to the other approaches examined, our outcomes for the proposed approach are qualitatively as well as quantitatively better.

5. CONCLUSION

This work presented a novel DLD: Deep Learning-Based Single Image De-Raining Using Discrete Hartley Transformation technique to improve image efficiency. Initially, the data are cleansed by Contrast limited adaptive histogram equalization which reduces the noise and smoothens the image. Moreover, this research introduced a new method to reconstruct a rainy image called Discrete Hartley Transformation (DHT). Following that, to extract the features this research proposed a Deep Learning-based Enhanced Share-Source Residual Module (SSRM) that improves image performance also its shortcut connections. To improve the accuracy, we introduced Enhanced SSRM which comprises Group normalization (GN) and Sigmoid function that smooth the gradient, much more flexible and better to handle. Finally, the Inverse Discrete Hartley Transformation (IDHT) is used to de-rained images. In comparison to the current methods, the approach we propose delivers great accuracy, efficiency, and time savings.

REFERENCES

[1] Fu, X., Huang, J., Ding, X., Liao, Y., & Paisley, J. Clearing the skies: A deep network architecture for single-image rain removal. IEEE Transactions on Image Processing 2017; 26(6): 2944-2956.
[2] Fu, X., Huang, J., Zeng, D., Huang, Y., Ding, X., & Paisley, J. Removing rain from single images via a deep detail network. In Proceedings of the IEEE conference on computer vision and pattern recognition 2017: 3855-3863.
[3] He, K., Zhang, X., Ren, S., Sun, J. Deep residual learning for image recognition. arXiv:1512.03385 2015.
[4] Shen, L., Yue, Z., Chen, Q., Feng, F., & Ma, J. Deep joint rain and haze removal from a single image. In 2018 24th International Conference on Pattern Recognition (ICPR) 2018: 2821-2826.
[5] Haar, A. Zur theorie der orthogonalen funktionensysteme. Georg-August-Universitat, Gottingen 1999.
[6] He, K., Sun, J., & Tang, X. Single image haze removal using dark channel prior. IEEE transactions on pattern analysis and machine intelligence 2010; 33(12): 2341-2353.
[7] Li, Y., Tan, R. T., Guo, X., Lu, J., & Brown, M. S. Rain streak removal using layer priors. In Proceedings of the IEEE conference on computer vision and pattern recognition 2016: 2736-2744.
[8] Li, Y., Tan, R.T., Guo, X., Lu, J., & Brown, M.S. Single image rain streak decomposition using layer priors. IEEE Transactions on Image Processing 2017; 26(8): 3874-3885.
[9] Zhu, L., Fu, C. W., Lischinski, D., & Heng, P. A. Joint bi-layer optimization for single-image rain streak removal. In Proceedings of the IEEE international conference on computer vision 2017: 2526-2534.
[10] Zhang, H., & Patel, V. M. Convolutional sparse and low-rank coding-based rain streak removal. In 2017 IEEE Winter conference on applications of computer vision (WACV) 2017: 1259-1267.
[11] Chen, D. Y., Chen, C. C., & Kang, L. W. Visual depth guided color image rain streaks removal using sparse coding. IEEE transactions on circuits and systems for video technology 2014; 24(8): 1430-1455.
[12] Huang, D.A., Kang, L.W., Wang, Y.C.F., & Lin, C.W. Self-learning based image decomposition with applications to single image denoising. IEEE Transactions on multimedia 2013; 16(1): 83-93.
[13] Kang, L.W., Lin, C.W., & Fu, Y.H. Automatic single-image-based rain streaks removal via image decomposition. IEEE transactions on image processing 2011; 21(4): 1742-1755.
[14] Park, K., Yu, S., & Jeong, J. A contrast restoration method for effective single image rain removal algorithm. In 2018 International workshop on advanced image technology (IWAIT) 2018: 1-4.
[15] Yu, S., Ou, W., You, X., Mou, Y., Jiang, X., & Tang, Y. Single image rain streaks removal based on self-learning and structured sparse representation. In 2015 IEEE China Summit and international conference on signal and information processing (chinaSIP) 2015: 215-219.

[16] Chang, Y., Yan, L., & Zhong, S. Transformed low-rank model for line pattern noise removal. In Proceedings of the IEEE international conference on computer vision 2017: 1726-1734.
[17] Chen, Q., Yi, X., Ni, B., Shen, Z., & Yang, X. Rain removal via residual generation cascading. In 2017 IEEE Visual Communications and Image Processing (VCIP) 2017: 1-4.
[18] Goodfellow, I., Pouget-Abadie, J., Mirza, M., Xu, B., Warde-Farley, D., Ozair, S., & Bengio, Y. Generative adversarial nets. Advances in neural information processing systems 2014; 27.
[19] Gu, S., Meng, D., Zuo, W., & Zhang, L. Joint convolutional analysis and synthesis sparse representation for single image layer separation. In Proceedings of the IEEE international conference on computer vision 2017: 1708-1716.
[20] Yang, W., Tan, R. T., Feng, J., Liu, J., Guo, Z., & Yan, S. Deep joint rain detection and removal from a single image. In Proceedings of the IEEE conference on computer vision and pattern recognition 2017: 1357-1366.
[21] Yang, W., Tan, R. T., Feng, J., Liu, J., Guo, Z., & Yan, S. Deep joint rain detection and removal from a single image. In Proceedings of the IEEE conference on computer vision and pattern recognition 2017: 1357-1366.
[22] Ren, W., Tian, J., Han, Z., Chan, A., & Tang, Y. Video desnowing and deraining based on matrix decomposition. In Proceedings of the IEEE conference on computer vision and pattern recognition 2017: 4210-4219.
[23] Wang, Y., Chen, C., Zhu, S., & Zeng, B. A framework of single-image deraining method based on analysis of rain characteristics. In 2016 IEEE International conference on image processing (ICIP) 2016: 4087-4091.
[24] Shen, L., Yue, Z., Chen, Q., Feng, F., & Ma, J. Deep joint rain and haze removal from a single image. In 2018 24th International Conference on Pattern Recognition (ICPR) 2018: 2821-2826.
[25] Zhou, M., Xiao, J., Chang, Y., Fu, X., Liu, A., Pan, J., & Zha, Z. J. Image de-raining via continual learning. In Proceedings of the IEEE/CVF Conference on Computer Vision and Pattern Recognition 2021: 4907-4916.
[26] Fu, X., Qi, Q., Zha, Z.J., Ding, X., Wu, F., & Paisley, J. Successive graph convolutional network for image de-raining. International Journal of Computer Vision 2021; 129: 1691-1711.
[27] Yang, F., Ren, J., Lu, Z., Zhang, J., & Zhang, Q. Rain-component-aware capsule-GAN for single image de-raining. Pattern Recognition 2022; 123: 108377.
[28] Xiao, J., Fu, X., Liu, A., Wu, F., & Zha, Z.J. Image de-raining transformer. IEEE Transactions on Pattern Analysis and Machine Intelligence 2022.
[29] Yao, G., Wang, C., Wu, Y., & Wang, Y. Pyramid fully residual network for single image de-raining. Neurocomputing 2021; 456: 168-178.
[30] Zhang, Z., Zhu, Y., Fu, X., Xiong, Z., Zha, Z. J., & Wu, F. Multifocal attention-based cross-scale network for image de-raining. In Proceedings of the 29th ACM International Conference on Multimedia 2021; 3673-3681.
[31] Wang, P., & Zhu, H. Single-image de-raining using joint filter and multi-scale deep alternate-connection dense network. Neurocomputing 2021; 457: 306-321.
[32] Wei, B., Zhang, L., Wang, K., Kong, Q., & Wang, Z. Dynamic scene deblurring and image de-raining based on generative adversarial networks and transfer learning for internet of vehicle. EURASIP Journal on Advances in Signal Processing 2021: 1-19.